Do Bony Orbit Dimensions Predict Diel Activity Pattern in Sciurid Rodents?

STEPHANIE M. SMITH,[1*] KENNETH D. ANGIELCZYK,[2] LARS SCHMITZ,[3] AND STEVE C. WANG[4]

[1]Department of Biology and Burke Museum of Natural History and Culture, University of Washington, Seattle, Washington
[2]Integrative Research Center, Field Museum of Natural History, Chicago, Illinois
[3]W.M. Keck Science Department, Claremont McKenna, Pfizer, and Scripps Colleges, Claremont, California
[4]Department of Mathematics and Statistics, Swarthmore College, Swarthmore, Pennsylvania

ABSTRACT

Diel activity pattern (DAP) is a key aspect of an animal's ecology, but it is difficult to infer when behavior cannot be directly observed, as in the fossil record. Various anatomical correlates have therefore been used to attempt to classify DAP. Eyeball dimensions are good predictors of DAP because they relate directly to light sensitivity of the eye. Osteological characters, such as scleral ring dimensions, are also reliable proxies, but bony orbit dimensions alone have proven less reliable because soft tissues other than the eyeball can affect orbit size and shape. However, it would be useful if bony orbit dimensions could be used to determine DAP, particularly for mammals, which have no scleral ring, and nonmammalian synapsids, which infrequently preserve scleral rings. We investigated the possibility of predicting DAP in sciurids (Mammalia: Rodentia: Sciuridae) using orbit measurements and other cranial dimensions, and a variety of quantitative methods, including phylogenetic flexible discriminant analysis, classification trees, and logistic regression. The latter two methods do not require *a priori* assignment of DAP and therefore reflect the situation in a fossil data set. We find that although there are some interfering phylogenetic factors, nocturnal and non-nocturnal sciurids can be differentiated from one another with over 80% accuracy using all methods investigated here; attempts to differentiate crepuscular animals from nocturnal and diurnal species proved much less successful. Our results indicate that these analyses offer several viable options for predicting DAP in the fossil record, but such analyses should be conducted in a phylogenetic context whenever possible. Anat Rec, 301:1774–1787, 2018. © 2018 Wiley Periodicals, Inc.

Key words: mammals; diel activity pattern; orbit dimensions; morphometrics; sciurids; phylogenetic comparative methods

Additional Supporting Information may be found in the online version of this article.

Grant sponsor: National Science Foundation; Grant number: DEB-0849958.

*Correspondence to: Stephanie M. Smith, Department of Biology and Burke Museum of Natural History and Culture, University of Washington, 24 Kincaid Hall, Box 351800, Seattle, WA 98195 E-mail: ssmith7@uw.edu

Received 24 August 2017; Revised 9 March 2018; Accepted 17 March 2018.

DOI: 10.1002/ar.23900
Published online 17 October 2018 in Wiley Online Library (wileyonlinelibrary.com).

Diel activity pattern (DAP) is a key aspect of an animal's ecology and behavior. The periods of the day or night during which an animal is active influence the resources available to it, its foraging habits, and the potential predators it may encounter. DAP also plays an important role in temporal and spatial resource partitioning in an ecosystem (Schoener, 1974; Kronfeld-Schor and Dayan, 2003). Because diurnal and nocturnal animals face different selective regimes, their sensory physiologies can differ significantly. For animals that rely primarily on vision to collect information about their environment, selection reflecting the contrasting characteristics of photopic (brightly lit) and scotopic (dimly lit) settings can ultimately result in different characteristics of the eye. In particular, the ability of eyes to produce bright images even in dim light conditions is considered a driving factor in the morphological evolution of eyes (Kirk, 2006; Hall and Ross, 2007; Hall, 2008a, 2008b; Schmitz and Wainwright, 2011).

The selective benefit of light-sensitive eyes varies with the light intensity of the preferred time of activity over the 24-hr cycle, because natural irradiance levels in terrestrial environments span eight to nine orders of magnitude (Lythgoe, 1979; Land, 1981; Martin, 1983). Physiological optics predicts several modifications of the optical system of amniote eyes that would increase visual light sensitivity. Given a fixed number of photoreceptors, an amniote eye adapted to a dim light environment should have (1) a large pupil diameter (aperture of the optical system) relative to posterior nodal distance (distance from near the center of the lens to the retina) to increase retinal image brightness and (2) a large pupil diameter relative to retinal area to maximize the number of photons entering the eye (Schmitz and Motani, 2010). Building on a large body of literature, Schmitz and Motani (2010) introduced the optical ratio $LD^2/ED \times AL$ (LD = lens diameter; ED = eyeball diameter; AL = axial length), where lens diameter is a proxy for pupil diameter, axial length, a proxy for posterior nodal distance, and eye diameter, a proxy for retinal area. A large optical ratio, with a large pupil and lens for given eye dimensions, would be advantageous in a scotopic environment, where light is scarce.

Differences in gross eyeball morphology between diurnal and nocturnal species have been quantified in several groups of amniotes, including mammals (Brooke et al., 1999; Ross, 2000; Thomas et al., 2002, 2004, 2006; Clement, 2004; Kirk, 2004, 2006; Werner and Seifan, 2006; Hall and Ross, 2007; Ross and Kirk, 2007; Hall, 2008a, 2008b, 2009; Schmitz, 2009). Schmitz and Motani (2010) showed that amniotes of different DAP can be differentiated with high reliability based on gross eyeball morphology, without information on the structure and composition of the retina; this distinction is much less clear within mammals, however (Hall et al., 2012). Previous research has shown that the well-ossified orbits of primates do allow some predictions of the dimensions of the eyes and DAP (Kay and Kirk, 2000; Ross and Kirk, 2007; although see Kirk, 2006), but this may not be possible across all mammalian clades (Pihlström, 2012) in part because mammalian eye shapes do not vary with DAP in a manner similar to other vertebrates (Hall et al., 2012).

Using osteological correlates to infer the light sensitivity of the eye is also problematic in mammals because they do not have a scleral ring, which has proven critical to correlation between eye dimensions and DAP in other extant and extinct amniotes (Schmitz, 2009; Schmitz and Motani, 2010, 2011a, 2011b; Angielczyk and Schmitz, 2014). This means that any attempt to reconstruct DAP in extinct mammals must be based solely on bony orbit and skull dimensions. Yet, if DAP could be reconstructed accurately in this way, it would allow this character to be studied in a wide variety of extinct mammals, which in turn would provide a more complete picture of the evolutionary history of light sensitivity, and likely DAPs among mammals and their extinct relatives (nonmammalian synapsids). Estimated DAPs of fossil mammals would be particularly useful for directly testing the nocturnal bottleneck hypothesis of mammalian evolution, which is mostly based on information from living species.

Here we test the utility of bony orbit and skull dimensions for predicting DAP using a modern mammalian clade, the sciurid rodents (family Sciuridae), as a case study. Sciurids are an ideal test clade for this investigation because they are species-rich and ecologically diverse, displaying the full spectrum of DAP and occupying a broad range of habitats and dietary niches. We also chose to focus on sciurids because they have a relatively poorly defined bony orbit, with a posterior boundary approximated only by a short postorbital process, in contrast to the well-defined orbit and complete postorbital bar of primates. Although a variety of 3D methods have been used to connect DAP to bony orbit dimensions and features, eyeball size, and eyeball orientation (Heesy, 2004, 2008; Ross et al., 2007; Rosenberger et al., 2016), we use only linear measurements, which have clear relationships with eyeball properties (Schmitz, 2009), are easy to identify on the sciurid skull, and do not require costly and time-consuming 3D scans.

First, we investigate the relationship between orbit and skull dimensions and activity patterns in sciurids, and whether these dimensions can be used in discriminant function analysis to differentiate among DAP categories. We then attempt to predict DAP in sciurids using classification trees and logistic regression, neither of which requires *a priori* assignment of DAP; this reflects the situation in fossil data sets, wherein the number of DAP groups present is unknown. If nocturnal, diurnal, and crepuscular sciurids can be correctly classified using these methods, they may be useful for reconstructing DAP in a variety of extinct mammalian groups.

MATERIALS AND METHODS

Taxonomic Sampling

We collected orbit and cranial measurements from 429 specimens of rodents in the family Sciuridae (squirrels). Our data set includes 51 of the 272 species comprising the family, and 29 of 51 total genera (Table 1; Nowak, 1999). All specimens were obtained from the collections of Field Museum of Natural History (FMNH). Most genera were represented by a single species. For each included species, we took measurements on 10 specimens wherever possible; some species with fewer than 10 available specimens were included to improve the phylogenetic or ecological breadth of the sample. In the case of nocturnal species, we frequently had to include more than one species per genus to have about 10 representatives of the genus in the data set. We excluded from our sample

TABLE 1. Diel activity pattern, diet, and habitat of taxa included in this study

Species	Diel activity pattern (DAP)	Diet	Habitat	References
Aeromys thomasi	Nocturnal	Seeds, fruit, arthropods	Forest	Nowak, 1999
Ammospermophilus leucurus	Diurnal	Seeds, fruit, arthropods, carrion	Arid plains, mountain slopes	Nowak, 1999
Belomys pearsonii	Nocturnal	Leaves, needles, fruit	Forest	Thorington et al., 2012
Callosciurus notatus	Diurnal	Plant matter, arthropods, eggs	Forest	Nowak, 1999
Callospermophilus lateralis	Diurnal	Plant matter, arthropods, eggs, small vertebrates	Prairie, steppe, desert	Nowak, 1999
Cynomys ludovicianus	Diurnal	Grasses, herbs	Plains, plateaus	Nowak, 1999
Dremomys lokriah	Diurnal	Seeds, fruit, arthropods	Forest	Molur et al., 2005; Thorington et al., 2012
Eoglaucomys fimbriatus	Nocturnal	Seeds, leaves	Forest	Nowak, 1999
Exilisciurus concinnus	Diurnal	Plant matter	Forest	Abaño et al., 2011; Nowak, 1999
Funambulus pennantii	Diurnal	Plant matter, arthropods	Forest	Nowak, 1999
Funisciurus congicus	Crepuscular/ cathemeral	Seeds, fruit, arthropods, eggs	Forest, scrub, savannah	Nowak, 1999
Funisciurus isabella	Crepuscular/ cathemeral	Seeds, fruit, arthropods, eggs	Forest, scrub, savannah	Nowak, 1999
Glaucomys sabrinus	Nocturnal	Seeds, fruits, fungi	Forest	Nowak, 1999
Glaucomys volans	Nocturnal	Seeds, fruits, fungi	Forest	Nowak, 1999
Heliosciurus gambianus	Crepuscular/ cathemeral	Seeds, fruit, arthropods, eggs	Forest, savannah	Nowak, 1999
Heliosciurus rufobrachium	Crepuscular/ cathemeral	Seeds, fruit, arthropods, eggs	Forest, savannah	Nowak, 1999
Hylopetes alboniger	Nocturnal	Plant matter, arthropods	Forest	Nowak, 1999
Hylopetes nigripes	Nocturnal	Plant matter, arthropods	Forest	Nowak, 1999
Hylopetes phayrei	Nocturnal	Plant matter, arthropods	Forest	Nowak, 1999
Hylopetes spadiceus	Nocturnal	Plant matter, arthropods	Forest	Nowak, 1999
Ictidomys tridecemlineatus	Diurnal	Plant matter, arthropods, eggs, small vertebrates	Prairie, steppe, desert	Nowak, 1999
Iomys horsfieldii	Nocturnal	Fruit	Forest	Chua et al., 2013; Thorington Jr et al., 2012
Marmota caligata	Diurnal	Plant matter	Steppe, meadow	Nowak, 1999
Marmota flaviventris	Diurnal	Plant matter	Steppe, meadow	Nowak, 1999
Marmota monax	Diurnal	Plant matter	Steppe, meadow	Nowak, 1999
Microsciurus flaviventer	Diurnal	Arthropods, bark, fungi	Forest	Jessen et al., 2016
Paraxerus cepapi	Crepuscular/ cathemeral	Seeds, fruit	Forest	Nowak, 1999
Petaurista elegans	Nocturnal	Seeds, fruit, leaves	Forest	Nowak, 1999
Petaurista magnificus	Nocturnal	Seeds, fruit, leaves	Forest	Nowak, 1999
Petaurista petaurista	Nocturnal	Seeds, fruit, leaves	Forest	Nowak, 1999
Petinomys crinitus	Nocturnal	Seeds, fruit, leaves	Forest	Nowak, 1999
Petinomys hageni	Nocturnal	Seeds, fruit, leaves	Forest	Nowak, 1999
Protoxerus stangeri	Diurnal	Seeds, fruit	Forest	Thorington Jr et al., 2012
Pteromys volans	Nocturnal	Seeds, fruit, bark	Forest	Nowak, 1999
Ratufa affinis	Crepuscular/ cathemeral	Seeds, fruit	Forest	Thorington Jr et al., 2012
Ratufa bicolor	Crepuscular/ cathemeral	Seeds, fruit	Forest	Thorington Jr et al., 2012
Sciurus carolinensis	Crepuscular/ cathemeral	Seeds, fruit	Forest	Nowak, 1999
Sciurus deppei	Diurnal	Seeds, fruit	Forest	Thorington Jr et al., 2012
Sciurus oculatus	Crepuscular/ cathemeral	Seeds, fruit	Forest	Best, 1995; Nowak, 1999
Spermophilopsis leptodactylus	Crepuscular/ cathemeral	Seeds, fruit, plant matter, arthropods	Desert	Nowak, 1999
	Diurnal	Seeds, fruit, arthropods	Forest	Thorington et al., 2012

(Continues)

TABLE 1. Continued

Species	Diel activity pattern (DAP)	Diet	Habitat	References
Sundasciurus hippurus				
Tamias alpinus	Diurnal	Plant matter, arthropods, eggs, fungi	Forest, plains	Nowak, 1999
Tamias amoenus	Diurnal	Plant matter, arthropods, eggs, fungi	Forest, plains	Nowak, 1999
Tamias panamintinus	Diurnal	Plant matter, arthropods, eggs, fungi	Forest, plains	Nowak, 1999
Tamiasciurus hudsonicus	Crepuscular/ cathemeral	Plant matter, arthropods, eggs, fungi, small vertebrates	Forest	Nowak, 1999
Tamiops macclellandii	Diurnal	Fruit, seeds, arthropods	Forest	Nowak, 1999
Trogopterus xanthipes	Nocturnal	Fruit, seeds, leaves	Forest	Nowak, 1999
Urocitellus elegans	Diurnal	Plant matter, arthropods, eggs, small vertebrates	Prairie, steppe, desert	Nowak, 1999
Urocitellus richardsonii	Diurnal	Plant matter, arthropods, eggs, small vertebrates	Prairie, steppe, desert	Nowak, 1999
Xerus erythropus	Diurnal	Plant matter, arthropods, eggs, small vertebrates	Grassland	Nowak, 1999
Xerus inauris	Diurnal	Plant matter, arthropods, eggs, small vertebrates	Grassland	Nowak, 1999

specimens with obvious pathologies, broken specimens, and juveniles.

Assignment of Ecology and Diel Activity Pattern

We used information from the primary literature (Table 1) to assign each sciurid species to one of three diel activity pattern groups: nocturnal (active primarily in a scotopic environment), diurnal (active primarily in a photopic environment), or crepuscular/cathemeral. We combined crepuscular (active at dawn and dusk) and cathemeral (equally likely to be active at any time of day) patterns because both include animals that are active in varying or intermediate light levels (mesopic environment).

We classified species based on qualitative information from the literature. For example, we found sciurids in the genus *Tamias* reported as being "strictly diurnal" (Nowak, 1999: 1250) and therefore assigned them to the diurnal group. However, other genera and species did not have such straightforward designations. *Tamiasciurus hudsonicus* is reported as being "basically diurnal" but is observed to have "two periods of intense activity, one just after dawn and another during the late afternoon in summer and around noon in winter" (Nowak, 1999: 1272, citing Ferron, 1976). Because this is indicative of activity in mesopic environments (*e.g.*, just after dawn), we classified *T. hudsonicus* as crepuscular/cathemeral. In addition to DAP information, we collected general diet and habitat information (Table 1) to rule out the possibility that morphological differences among species might arise from those factors instead of DAP. Whenever possible, we sampled multiple DAPs within a habitat grouping; this was not possible in the case of arboreal gliders, all of which are nocturnal.

Cranial and Dental Measurements

We collected six linear measurements on each sciurid skull (Fig. 1). Four measurements are directly related to orbit size (Table 2). We chose these measurements because they have clear relationships to eye properties that are directly related to visual light sensitivity (Schmitz, 2009). We chose not to include optic nerve foramen area. Although this measurement varies with DAP in primates (Kay and Kirk, 2000), it is difficult to measure accurately on very small specimens, and is preserved in fossil taxa relatively infrequently (Kay and Kirk, 2000), rendering it less useful for predicting DAP in a fossil data set. We measured two body size proxies on the skull (skull length and height); we also measured length and width of upper and lower first molars (M1/m1) and multiplied them together to obtain M1/m1 area for two additional body size proxies. All measurements were collected with digital calipers to 0.1 mm accuracy.

Phylogenetic Framework and Ancestral State Reconstruction

Wherever possible, we conducted our analyses using phylogenetically informed statistics. Our data violate the assumption of phylogenetic independence, and it is therefore appropriate to account for that fact in our analyses and only report phylogenetically corrected results (see Freckleton, 2009 for further discussion of this issue). Except as otherwise noted, all the following analyses were conducted in R version 3.3.1 and 3.4.0 (R Core Team, 2016). For phylogenetic comparative methods, we pruned the species-level tree of Bininda-Emonds et al. (2007) to include only our sampled species, randomly resolved all polytomies, and for computation purposes, scaled zero-length branches to be $1.0e^{-6}$ of the total tree length (Fig. 2). We further updated the taxonomic nomenclature within the genus *Spermophilus* to reflect recent revisions (Helgen et al., 2009). Although this approach results in paraphyly of the genus *Urocitellus*, it does not have an unreasonable effect on our particular analyses, as there are no shifts in DAP among species within the Marmotini. Using SIMMAP functions from the

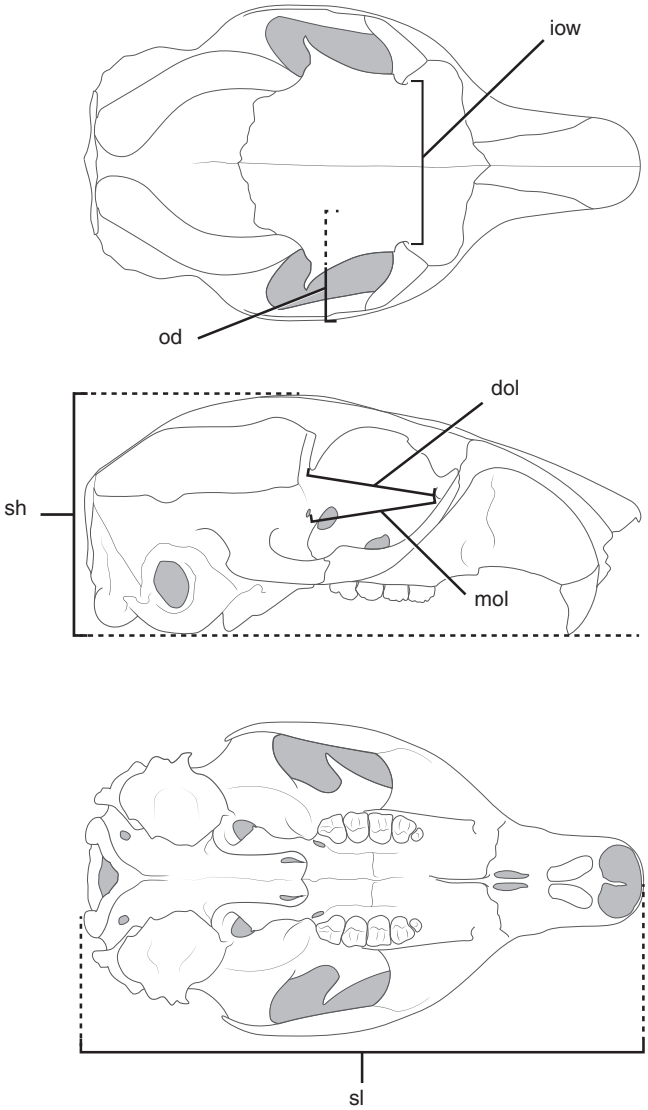

Fig. 1. Cranial measurements used in this study. All measurements are shown on skull of *Sciurus carolinensis* and described in Table 2. Dental measurements not shown. Abbreviations: iow = interorbital width; od = orbit depth; dol = diagonal orbit length; mol = maximum orbit length; sh = skull height; sl = skull length.

R package phytools (Revell, 2012), we reconstructed ancestral states of DAP with three different transition rate models: an equal rates model (ER) and two different models with transition matrices estimated based on likelihood, one with symmetrical rates (SYM), and one with all rates different (ARD). Model selection was performed using the Akaike Information Criterion (AIC). All simulations were run for 1,000 generations.

Differentiation of DAP Categories

To investigate basic correlations between DAP, body size, and orbit dimensions, we conducted phylogenetic generalized least squares (PGLS) regression on several combinations of log-transformed species averages of orbit dimensions and body size proxies. PGLS regressions were executed using functions from phytools (Revell, 2012), with two models of evolution: a Brownian motion model (BM) and an Orstein-Uhlenbeck model (OU; Hansen, 1997). Alpha and lambda were estimated using maximum likelihood. After diagnostic PGLS regressions to determine if there were any outliers in our data, we tested for significant differences among PGLS residuals of the three DAP categories, as well as between nocturnal and non-nocturnal (= crepuscular/cathemeral and diurnal lumped together) groups only. We were unable to use parametric tests because in many cases the PGLS residuals violated the assumption of normality or homoscedasticity. We therefore made comparisons among the three DAP categories using the Kruskal–Wallis test, and between nocturnal and non-nocturnal groups using the Wilcoxon rank-sum test.

TABLE 2. Measurements taken for this study and relevant eyeball or body size proxies they represent

Measurement	Description	Proxy
Diagonal orbit length (DOL)	Distance from lacrimal foramen to posteroventral tip of postorbital process	Eyeball diameter
Maximum orbit length (MOL)	Distance from lacrimal foramen to sphenorbital fissure	Eyeball diameter
Orbit depth (OD)	Perpendicular distance from medial surface of zygomatic arch to optic nerve foramen	Axial eyeball length
Interorbital width (IOW)	Minimum distance between orbits measured on dorsal side of skull (minimum width of frontals)	Degree of orbital convergence
Skull length (SL)	Distance from anterior end of premaxilla to posterior end of occipital condyles along ventral surface	Body size
Skull height (SL)	Maximum height of skull measured with skull placed ventral side down on a flat surface	Body size
Upper M1 area (UM1)	Length times width of M1	Body size
Lower m1 area (LM1)	Length times width of m1	Body size

Measurements are also depicted in Figure 1. Proxies are from Schmitz (2009).

To test if orbit dimensions can be used to determine DAP, we conducted phylogenetic flexible discriminant analysis (pFDA) with code from Motani and Schmitz (2011) (https://github.com/lschmitz/phylo.fda). We used log-transformed species average data and executed pFDA with a variety of variable combinations, with different types and numbers of body size proxies included in the analysis, to determine which combination of variables was the most successful at discriminating among activity patterns (combinations shown in Table 6).

Classification Tree and Logistic Regression

In fossil data sets, we typically want to predict the unknown DAPs of a group of species or individuals. We therefore sought to test how well we could predict DAP in a set of extant sciurids without prior information about

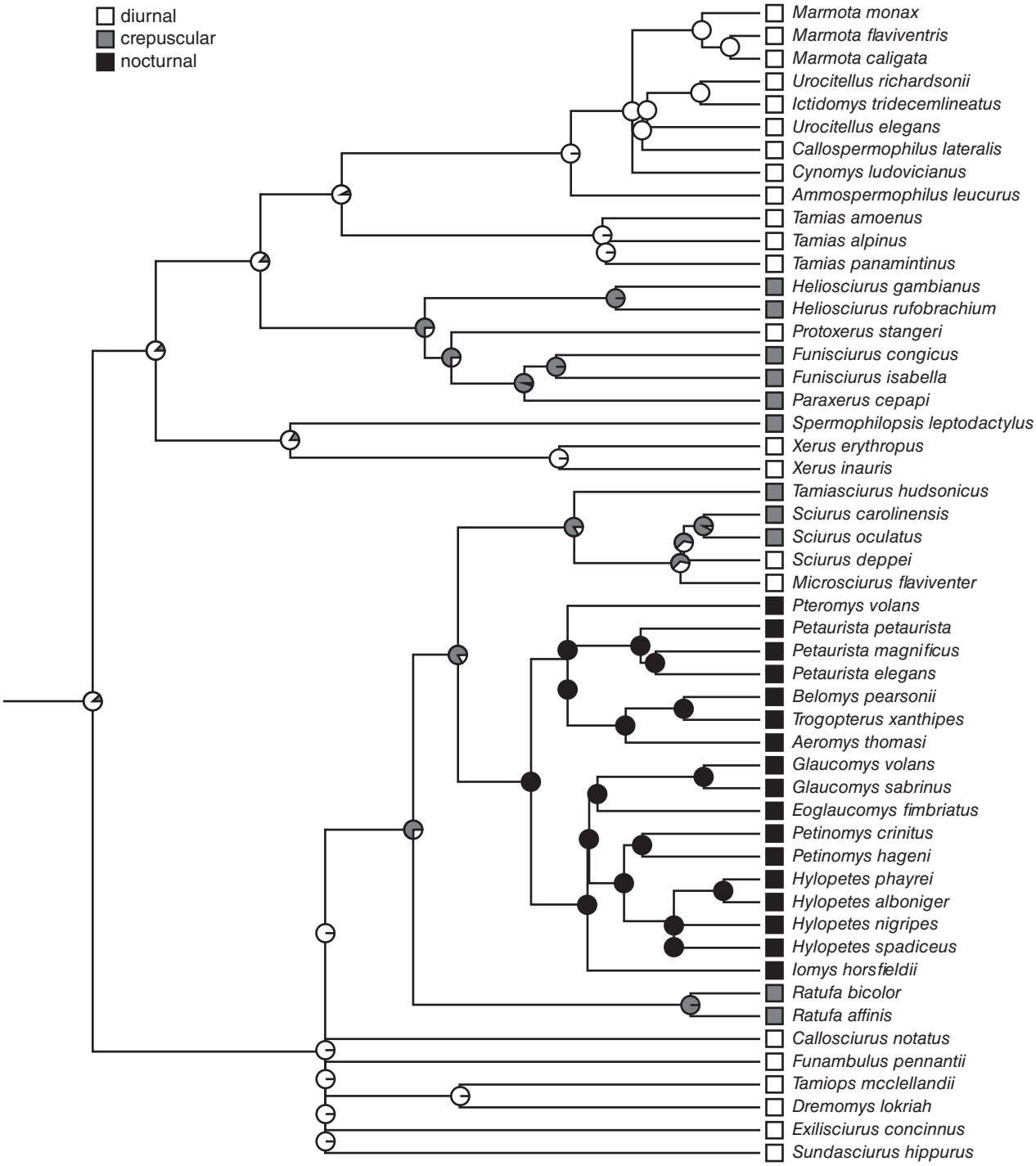

Fig. 2. Pruned phylogeny used in this study. Pie charts at nodes represent posterior probabilities of ancestral DAP character state, based on SIMMAP reconstruction with symmetrical transition matrix estimated using maximum likelihood. Colored squares at branch tips correspond to each species' DAP as found in the literature (Table 1).

the identity or number of DAPs represented in the data set. To do this, we used classification trees (also known as CART; Breiman et al., 1984) and logistic regression to predict DAP from skeletal and orbital measurements (R code available in Supporting Information). Classification trees attempt to predict DAP based on the results of a series of yes/no questions, such as "was the interorbital width greater than or equal to 13 mm?" Logistic regression is analogous to linear regression but is used to predict a categorical outcome such as DAP

rather than a continuous outcome. We ran classification trees using all nontransformed skeletal and orbital variables (Table 2) with both individual measurements and species averages. Log-transforming the variables does not affect results using classification trees, so we used nontransformed variables for ease of interpretation. These analyses were carried out using functions from the R packages rpart (Therneau and Atkinson, 2017) and rpart.plot (Milborrow, 2016). Using the same set of variables, we conducted logistic regressions on the log-transformed data, using all skeletal and orbital variables and using orbital variables only. All analyses were carried out in two configurations: three possible DAPs (crepuscular/cathemeral, nocturnal, diurnal) and two possible DAPs (nocturnal, non-nocturnal). We additionally conducted phylogenetically informed logistic regression for two possible DAPs, using all skeletal and orbital variables as well as using orbital variables only, with the function phyloglm() from package phylolm (Ho and Ane, 2014), with 1,000 bootstrap replicates and the bound on the linear predictor (btol) set to 20. There does not currently appear to be an implementation of phylogenetically informed logistic regression for three possible outcomes.

RESULTS

Ancestral State Reconstructions

The pruned tree used in these analyses is shown in Figure 2. In tests of various models of transition rates (ER, SYM, and ARD, with SYM and ARD matrices estimated using likelihood), the location of DAP shifts on the tree was largely congruent across models. Figure 2 shows the reconstructions from the symmetrical rates model, which had the best AIC score (Table 3). All three transition models produced a tree with a non-nocturnal root node, with all except the ARD model predicting a diurnal root. The three models also agreed on the near-certainty of a nocturnal ancestor of *Pteromys* + *Iomys*, Tribe Pteromyini (node 80). Other internal nodes showed more variation in DAP reconstruction because unlike the nocturnal taxa, neither the crepuscular nor diurnal taxa form a monophyletic clade. Internal nodes reconstructed most frequently as crepuscular include the common ancestor of *Paraxerus* and *Heliosciurus* (node 66), the common ancestor of *Sciurus carolinensis* and *Sciurus oculatus* (node 79), and the common ancestor of *Ratufa affinis* and *Ratufa bicolor* (node 96). Transitions in DAP reconstructed on our tree include the following (Fig. 2): a transition from diurnal to crepuscular/cathemeral in the common ancestor of *Marmota* and *Paraxerus* (Tribes Marmotini, Protoxerini); a shift from diurnal to crepuscular/cathemeral in the common ancestor of the nocturnal clade and its crepuscular/cathemeral sister group (*Tamiasciurus* + *Microsciurus*, both within Tribe Sciurini); a shift from crepuscular/cathemeral to nocturnal in the ancestor of the nocturnal clade (Tribe Pteromyini; *Pteromys* + *Iomys*); and two shifts from crepuscular/cathemeral back to diurnal (in *Protoxerus stangeri* and the common ancestor of *Sciurus deppei* and *Microsciurus flaviventer*).

Phylogenetic Generalized Least Squares

In both three-DAP PGLS regressions (Table 4) and two-DAP PGLS regressions (Table 5), diagonal orbit length (DOL), maximum orbit length (MOL), and interorbital width (IOW) regressed on skull length (SL), skull height (SH), or lower m1 (LM1) resulted in residuals with significant differences between DAP groups. IOW also resulted in significantly different residuals among DAP groups when regressed on upper M1 (UM1). Orbit depth (OD) resulted in significantly different residuals among DAPs only when regressed on UM1. Differences in model fit between BM and OU models were slight and inconsistent across variable combinations: neither one was consistently a better fit in every case. In all regressions using IOW and DOL, the OU model was a better fit, but the other two orbit measurements favor different models with different body size proxies. In several cases, there was very little difference in fit between the two models (e.g., IOW regressed on SL).

Phylogenetic Flexible Discriminant Analysis

Optimal lambda for the various permutations of our data set ranged from 0.31 to 0.42 (Table 6), indicating the need for removal of a moderate degree of phylogenetic covariance, presumably stemming from the concentration of nocturnal taxa in a single clade. The maximum total percent of specimens correctly identified was 72.6% with three DAP groups, but 88.2% with only two DAP groups. With three DAP groups, maximum percent correct identifications within DAP groups was 63.6% in crepuscular/cathemeral species, 65.2% in diurnal species, and 94.1% in nocturnal species. With two groups, maximum percent correct identifications within DAP groups was 85.3% in non-nocturnal species and 94.1% in nocturnal species. Three-group pFDA performed optimally with the inclusion of all four orbit dimensions, both skull dimensions, and UM1 (Fig. 3). Two-group pFDA performed optimally with the inclusion of only the four orbit dimensions (Fig. 4). All taxa that were misclassified by two-group pFDA were also misclassified by three-group pFDA, except *Ictidomys tridecemlineatus.*

Classification Tree and Logistic Regression

With three possible DAP classes, 62% of individuals and 65% of species were correctly classified by the classification tree approach; with two possible classes, 92% of individuals and 84% of species were correctly classified (Figs. 5 and 6 and Table 7). The logistic regressions performed somewhat better (Table 8). Using three DAP categories, a multinomial logistic regression classified 74% of individuals and 84% of species correctly when all eight orbital, cranial, and dental variables (Table 1) were used as predictors. When only the three orbital variables were used, 61% of individuals and 67% of species were classified correctly. Results improved considerably when using

TABLE 3. SIMMAP model fitting

Model	AIC	AIC weight
ER	58.06	0.154
SYM	55.03	0.704
ARD	58.24	0.141

AIC weights and scores for SIMMAP transition rate models for location of shifts in DAP along our pruned phylogeny. Abbreviations: ER = equal rates; SYM = symmetrical rates; ARD = all rates different.

TABLE 4. Three-DAP PGLS regression results

Orbit dim.		Skull length		Skull height		Upper M1 area		Lower m1 area	
		BM	OU	BM	OU	BM	OU	BM	OU
DOL	*P* value	**0.0041**	**0.0015**	**0.0095**	**0.015**	0.20	0.36	**0.016**	**0.050**
	AIC	−183.65	−187.49	−176.96	−181.48	−195.43	−207.36	−190.79	−191.30
	slope	0.75 (0.04)	0.80 (0.04)	0.89 (0.06)	0.93 (0.05)	0.30 (0.02)	0.33 (0.003)	0.28 (0.02)	0.30 (0.01)
MOL	*P* value	**<0.0001**	**<0.0001**	**0.0013**	**0.0013**	0.20	0.20	**0.012**	**0.012**
	AIC	−231.22	−230.29	−205.46	−205.08	−210.80	−210.57	−208.71	−206.97
	slope	0.92 (0.03)	0.93 (0.03)	1.09 (0.04)	1.10 (0.04)	0.36 (0.01)	0.36 (0.01)	0.35 (0.01)	0.35 (0.01)
OD	*P* value	0.28	0.29	0.37	0.38	**0.047**	**0.040**	0.26	0.26
	AIC	−233.17	−231.17	−214.47	−212.54	−211.13	−216.40	−211.54	−211.98
	slope	0.96 (0.03)	0.96 (0.03)	1.14 (0.04)	1.14 (0.04)	0.38 (0.01)	0.38 (0.01)	0.36 (0.01)	0.36 (0.01)
IOW	*P* value	**<0.0001**	**<0.0001**	**<0.0001**	**<0.0001**	**<0.0001**	**<0.0001**	**<0.0001**	**<0.0001**
	AIC	−131.61	−131.78	−138.57	−139.32	−104.38	−108.43	−108.77	−111.62
	slope	1.00 (0.07)	1.00 (0.07)	1.23 (0.08)	1.21 (0.08)	0.36 (0.04)	0.36 (0.03)	0.36 (0.03)	0.35 (0.03)

PGLS regression results for various combinations of orbit dimensions regressed on body size proxies, with three DAP categories. Listed values are *P* values for Kruskal–Wallis test comparing PGLS residuals for crepuscular/cathemeral, diurnal, and nocturnal species, under both a Brownian Motion (BM) and Orstein-Uhlenbeck (OU) model.Significant *P* values in bold. Also reported are model AIC and slope (standard error in parentheses).
Abbreviations: DOL = diagonal orbit length; MOL = maximum orbit length; OD = orbit depth; IOW = interorbital width.

two DAP categories. A binomial logistic regression classified 95% of individuals and 100% of species correctly when all eight orbital, cranial, and dental variables were used as predictors. When only the three orbital variables were used, 83% of individuals and 90% of species were classified correctly. Phylogenetic logistic regression with two DAP categories performed similarly well; with three orbit variables, 88.2% of species were classified correctly.

DISCUSSION

Our main objectives in this study were (1) to determine how well bony orbit dimensions predict DAP in sciurid rodents, (2) to assess the degree to which the relationship between DAP and orbit size is influenced by phylogeny, and (3) to use our results to understand how our methods might be applied to determine DAP in the mammalian fossil record. We began with ancestral state reconstructions of DAP across the sciurid tree to detect shifts in DAP through the history of the clade. Our results indicate that it is very unlikely that the common ancestor of sciurids was nocturnal; this is probably due to the presence of the nocturnal taxa within a single highly nested clade, in contrast to the more scattered crepuscular/cathemeral and diurnal clades, with multiple inferred shifts between the two patterns (Fig. 2). This limits the number of phylogenetically independent tests of the relationship between DAP and orbit size because with only one transition to nocturnality, it is difficult to rigorously test the correlation between bony orbit size and the evolution of a nocturnal DAP. Roll et al. (2006) demonstrated that across Rodentia, more closely related species are more likely to have a similar DAP, indicating that there are some phylogenetic constraints on the plasticity of this trait that extend beyond the level of Sciuridae. However, our tree shows several transitions from the ancestral activity pattern (most likely diurnal) to a crepuscular/cathemeral DAP, and back again (Fig. 2), providing several potential independent tests of the relationship between DAP and orbit dimensions.

It is tempting to conclude from these results that a shift from diurnal to nocturnal is evolutionarily more "difficult" than a shift from diurnal to crepuscular/cathemeral and *vice versa.* If crepuscular/cathemeral animals have eyes that are morphologically intermediate between diurnal and nocturnal animals (Kirk, 2004, 2006), a switch from crepuscular/cathemeral to either diurnal or nocturnal would require a less drastic change than a switch between nocturnal and diurnal. However, this is an oversimplification of a complex set of ecological traits and behaviors. For example, all nocturnal sciurids are also arboreal gliders. Other arboreal gliders within Rodentia (Anomaluridae, scaly-tailed flying "squirrels" of uncertain phylogenetic affinity) comprise only nocturnal or

TABLE 5. Two-DAP PGLS regression results

Orbit dim.	Skull length		Skull height		Upper M1 area		Lower m1 area	
	BM	OU	BM	OU	BM	OU	BM	OU
DOL	**0.0013**	**0.00032**	**0.0021**	**0.0034**	0.088	0.19	**0.017**	**0.031**
MOL	**<0.0001**	**<0.0001**	**0.00015**	**0.00017**	0.080	0.080	**0.0024**	**0.0024**
OD	0.12	0.12	0.39	0.39	**0.032**	**0.026**	0.20	0.20
IOW	**<0.0001**	**<0.0001**	**<0.0001**	**<0.0001**	**<0.0001**	**<0.0001**	**<0.0001**	**<0.0001**

PGLS regression results for various combinations of orbit dimensions regressed on body size proxies, with two DAP categories. Listed values are *P* values for Wilcoxon rank-sum test comparing PGLS residuals for nocturnal and non-nocturnal species, under both a Brownian Motion (BM) and Orstein-Uhlenbeck (OU) model. Significant *P* values are in bold.
Abbreviations: DOL = diagonal orbit length; MOL = maximum orbit length; OD = orbit depth; IOW = interorbital width.

TABLE 6. Two- and Three-DAP pFDA results

	λ	Total % correct	Non-nocturnal		Nocturnal
			Diurnal	Crepuscular/cathemeral	
Three-DAP					
DOL+MOL + OD + IOW	0.34	64.7	43.5	**63.6**	**94.1**
DOL+MOL + OD + SL	0.38	56.9	47.8	**63.6**	64.7
DOL+MOL + OD + SL + SH	0.42	58.8	52.2	**63.6**	64.7
DOL+MOL + OD + SL + SH + IOW	0.32	64.7	47.8	**63.6**	88.2
DOL+MOL + OD + SL + SH + IOW + LM1	0.33	70.6	56.5	**63.6**	**94.1**
DOL+MOL + OD + SL + SH + IOW + UM1	0.32	**72.6**	**65.2**	54.6	**94.1**
All variables (orbit, cranial, dental)	0.31	68.6	60.9	54.6	88.2
Two-DAP					
DOL+MOL + OD + IOW	0.34	**88.2**	**85.3**		**94.1**
DOL+MOL + OD + SL	0.38	78.4	79.4		76.5
DOL+MOL + OD + SL + SH	0.42	82.4	**85.3**		76.5
DOL+MOL + OD + SL + SH + IOW	0.32	86.3	82.4		**94.1**
DOL+MOL + OD + SL + SH + IOW + LM1	0.33	86.3	82.4		**94.1**
DOL+MOL + OD + SL + SH + IOW + UM1	0.32	86.3	82.4		**94.1**
All variables (orbit, cranial, dental)	0.31	86.3	82.4		**94.1**

Highest percent correct for each DAP category (crepuscular/cathemeral, diurnal, nocturnal) and total are in bold. For crepuscular/cathemeral, N = 11 species; for diurnal, N = 23 species; for nocturnal, N = 17 species.
Abbreviations: DOL = diagonal orbit length; MOL = maximum orbit length; OD = orbit depth; IOW = interorbital width; SL = skull length; SH = skull height; LM1 = lower m1; UM1 = upper m1.

crepuscular taxa (Julliot et al., 1998), and other nonrodent arboreal gliders are usually nocturnal as well (e.g., colugos and gliding marsupials [within Phalangeridae, Pseudocheiridae and Petauridae]; Nowak, 1999). It is therefore difficult to extricate the locomotor style and habitat of arboreal gliders from their DAP, but this pattern suggests that the gliding lifestyle may be linked with nocturnality.

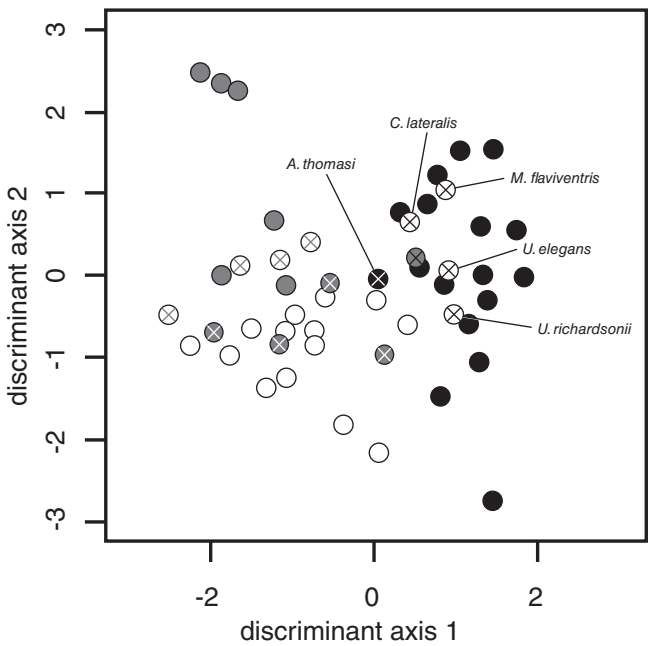

Fig. 3. Phylogenetic flexible discriminant analysis (pFDA) of all orbit measurements. Black points are nocturnal taxa, gray points are crepuscular/cathemeral taxa, and white points are diurnal taxa. Points marked with an X denote species misclassified by the pFDA; color of the X corresponds to the DAP predicted by pFDA. Labeled taxa are those that were also misclassified by two-DAP pFDA.

PGLS residuals (Tables 4 and 5) indicate that for a given body size, nocturnal sciurids have significantly larger bony orbits (MOL and DOL) than non-nocturnal sciurids. Because orbit length is closely correlated with eyeball diameter (Schmitz, 2009; MacIver et al., 2017), we interpret this as indicative of a significantly larger eye, and likely a larger pupil diameter, in nocturnal sciurids, which is consistent with optical principles and the advantages of a larger area for light capture when living in a scotopic environment (Schmitz and Motani, 2010, 2011a).

Two-DAP pFDA (Fig. 4 and Table 6) performed better than three-DAP pFDA (Fig. 3 and Table 6). All taxa misclassified in our two-DAP pFDA were also misclassified in our three-DAP pFDA (except *I. tridecemlineatus*), with several additional taxa being misclassified in the three-DAP analysis. In inspecting the predicted DAPs of the misclassified taxa, it is interesting to note that every taxon misclassified in only the three-DAP analysis (all labeled, Fig. 3) was predicted to be only one category away from its true DAP category, whereas those misclassified by the two-DAP analysis were nocturnal and classified as diurnal, or *vice versa.* To put it another way, if we consider a morphological continuum from diurnal to crepuscular/cathemeral to nocturnal, those taxa that were greater outliers (diurnal classified as nocturnal, *vice versa*) were misclassified irrespective of DAP group configuration; taxa that were on the border of crepuscular/cathemeral and diurnal or crepuscular/cathemeral and nocturnal were misclassified only by the more sensitive three-DAP model.

Interorbital width (IOW) residuals were significantly lower in nocturnal taxa than in diurnal and crepuscular/cathemeral taxa, irrespective of body size proxy used; this may be a signal of greater orbital convergence. Because all our nocturnal taxa are arboreal gliders, the increased degree of convergence we find might be correlated with a

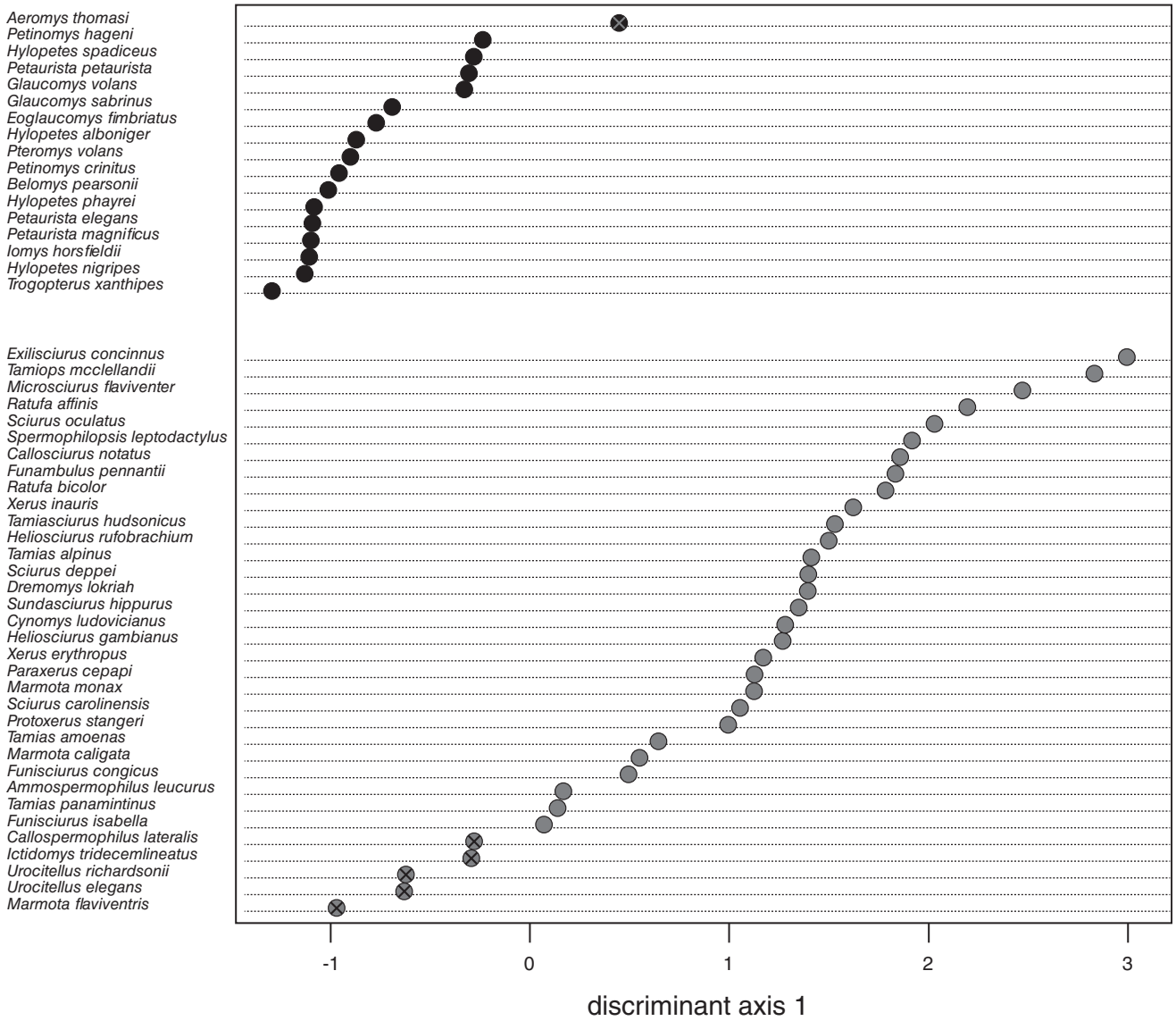

Fig. 4. Phylogenetic flexible discriminant analysis (pFDA) of all orbit, skull, and dental measurements except LM1. Black points are nocturnal taxa and gray points are non-nocturnal taxa. Points marked with an X denote species misclassified by the pFDA.

leafy environment and the advantages of binocular vision in a cluttered visual landscape (Changizi and Shimojo, 2008). However, of 10 non-nocturnal taxa with particularly low IOW residuals (in the range of nocturnal taxa), only three are forest-dwellers, whereas the other seven taxa favor arid environments or grasslands. Therefore, our present data do not allow us to conclude that increased orbital convergence is closely correlated with habitat in sciurids. Although the correlation of nocturnality with orbital convergence has been observed in nonprimate eutherian taxa (Heesy, 2008), and in this study, it is not universal. The degree to which orbital convergence alone is predictive of DAP is not clear based on our current findings; however, IOW is an important factor in our pFDA model for distinguishing nocturnal taxa. Indeed, of the five non-nocturnal taxa misclassified by two-category pFDA (Fig. 4), four have IOW residuals that are more negative than the mean IOW residual for nocturnal taxa.

It is possible that, rather than simply correlating with orbital convergence, low IOW is an additional manifestation of increased eye size, and reflects a skull-packing issue rather than adaptation for stereoscopic vision. However, all of the diurnal taxa with particularly low values for IOW are within the Marmotini (the monophyletic clade here bracketed by *Marmota* and *Tamias*), suggesting that this phenomenon is probably at least partially a phylogenetic signal, which persists even in the pFDA. These results highlight the need to conduct more investigations into the relationship between orbit position and nocturnality in nonprimate mammals, and to closely investigate the contribution of each variable when conducting a multivariate analysis of this type.

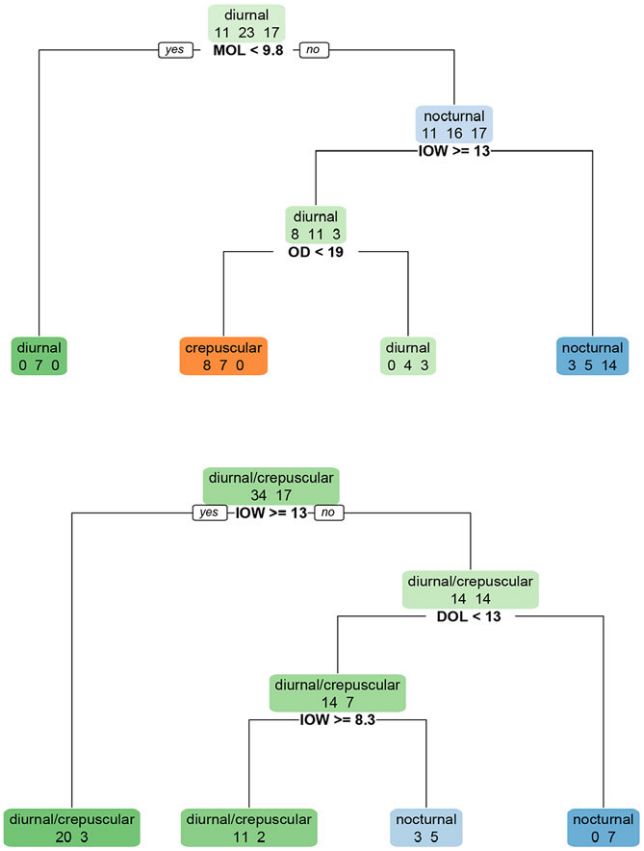

Fig. 5. Species-level classification tree using three (top) and two (bottom) DAP categories. For crepuscular/cathemeral, N = 11 species; for diurnal, N = 23 species; for nocturnal, N = 17 species. All eight orbital, cranial, and dental variables were eligible as predictors. Maximum depth was set to four levels. For each node, species satisfying the splitting criterion follow the left branch; species not satisfying the splitting criterion follow the right branch. Each terminal node gives the number of species falling into that node that are crepuscular/cathemeral, diurnal, and nocturnal for three-DAP tree (top), and non-nocturnal and nocturnal for two-DAP tree (bottom). For the three-DAP tree, green denotes nodes in which the most common DAP is diurnal, orange denotes nodes in which the most common DAP is crepuscular, and blue denotes nodes in which the most common DAP is nocturnal. For the two-DAP tree, green denotes nodes in which the most common DAP is non-nocturnal, and blue denotes nodes in which the most common DAP is nocturnal. Intensity of color corresponds to the purity (prediction accuracy) of each node. As results are identical whether or not the data are log-transformed, untransformed values are shown in the splitting criteria for ease of interpretation. Abbreviations: DOL = diagonal orbit length; MOL = maximum orbit length; OD = orbit depth; IOW = interorbital width.

Our results differ from previous analyses of broad amniote groups using pFDA (Schmitz and Motani, 2010, 2011a; Motani and Schmitz, 2011), where it was possible to distinguish among all three DAP categories using osteological correlates of eye size with ~80% accuracy (Schmitz and Motani, 2010; Angielczyk and Schmitz, 2014). However, these studies were conducted in animals that have scleral rings, which provide a very close approximation of the area of the eye aperture (Schmitz, 2009). Because mammals have no scleral ossicles, and sciurids have a postorbital process but lack the postorbital bar or plate possessed by primates and some other mammals, it is not surprising that sciurid bony orbit dimensions provided less DAP resolution than scleral ring measurements. Additionally, we did not account for any influence that the postorbital ligament might have on the shape of the postorbital process. The postorbital ligament is involved in withstanding biomechanical stresses on the skull during feeding in other mammals (Herring et al., 2011); in sciurids, these biomechanical demands could therefore have greater influence than eye size on the shape and length of the postorbital process.

There is a great deal of overlap in discriminant function space among species from the three DAP categories (Fig. 3 and Table 6). Our findings correspond with the findings of Hall et al. (2012), whose analyses used published soft tissue (eyeball) dimensions and found a much higher degree of correct classification in nocturnal mammals (92.4%) than in diurnal or crepuscular/cathemeral mammals (Hall et al., 2012: Table 6). Hall et al. (2012) did not carry out a two-DAP analysis, so we cannot compare our results in that situation. However, Hall et al. (2012) included diurnal anthropoid primates in their analysis, and noted that the

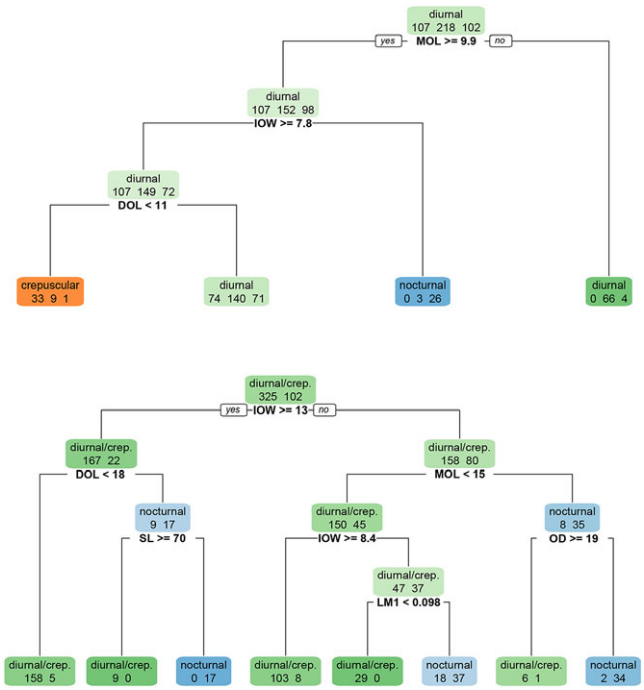

Fig. 6. Individual-level classification tree using three (top) and two (bottom) DAP categories. For crepuscular/cathemeral, N = 107 individuals; for diurnal, N = 218 individuals; for nocturnal, N = 102 individuals. All eight orbital, cranial, and dental variables were eligible as predictors. Maximum depth was set to four levels. For each node, species satisfying the splitting criterion follow the left branch; species not satisfying the splitting criterion follow the right branch. Each terminal node gives the number of species falling into that node that are crepuscular/cathemeral, diurnal, and nocturnal for three-DAP tree (top), and non-nocturnal and nocturnal for two-DAP tree (bottom). As results are identical, whether or not the data are log-transformed or untransformed values are shown in the splitting criteria for ease of interpretation. See Figure 5 caption for color code significance. Abbreviations: DOL = diagonal orbit length; MOL = maximum orbit length; OD = orbit depth; IOW = interorbital width; SL = skull length; LM1 = lower m1 area.

TABLE 7. Two- and three-DAP classification tree results

	Total % correct	Non-nocturnal		Nocturnal
		Diurnal	Crepuscular/ cathemeral	
Three-DAP				
Species-level	64.7	47.8	72.7	82.4
Individual-level	62.1	94.5	30.8	25.5
Two-DAP				
Species-level	84.3		91.1	70.6
Individual-level	92.0		93.8	86.3

Sample sizes for each species listed in Table 6. For crepuscular/cathemeral, N = 107 individuals; for diurnal, N = 218 individuals; for nocturnal, N = 102 individuals. Values are in-sample prediction rates using a single classification tree with a maximum depth of four levels.

very small relative corneal size of diurnal anthropoids was likely a factor in misclassification of what they class as "day-active non-anthropoids," whose relative corneal size range completely overlaps that of the nocturnal taxa included in the sample.

The fact that anthropoid primates have derived eye morphologies with particularly small corneal sizes (Ross, 2000; Kirk, 2004; Ross and Kirk, 2007) is frequently cited as a confounding factor in using eyeball dimensions to determine activity pattern. Further confounding this relationship is the negative allometry of primate eyeball size with respect to bony orbit size (Schultz, 1940; Kay and Cartmill, 1977; Kay and Kirk, 2000; Heesy and Ross, 2001). The nature of the allometric relationship between eyeball and bony orbit has not been studied extensively in nonprimate mammals, and further information would be necessary to determine if it has a significant effect when the bony orbit is poorly defined, as in sciurids. However, we find here that within sciurids, it is possible to use pFDA with bony orbit and body size dimensions to determine DAP (two categories, nocturnal and nonnocturnal), with greater than 85% accuracy. The inclusion of measurements other than eyeball measurements (e.g., IOW, discussed above) is likely providing additional information about orbital convergence that is not apparent when eyeball dimensions are used alone. If allometry is confounding our signal, it is not to a debilitating degree. Nevertheless, the relationship between soft tissue dimensions and the bony measurements used in this study should be further studied.

TABLE 8. Two- and three-DAP multinomial logistic regression results

	Total % correct	Non-nocturnal		Nocturnal
		Diurnal	Crepuscular/ cathemeral	
Three-DAP				
DOL+MOL + OD, species-level	66.7	82.6	0.0	88.2
All variables (orbit, cranial, dental), species-level	84.3	91.3	45.5	100.0
DOL+MOL + OD, indiv.-level	61.1	86.2	6.5	64.7
All variables (orbit, cranial, dental), indiv.-level	73.6	83.9	38.3	89.6
Two-DAP				
DOL+MOL + OD, species-level	90.2		94.1	82.4
All variables (orbit, cranial, dental), species-level	100.0		100.0	100.0
DOL+MOL + OD, indiv.-level	83.1		93.8	49.0
All variables (orbit, cranial, dental), indiv.-level	95.2		97.2	88.5

Sample sizes for each category listed in Tables 6 and 7. Values are in-sample prediction rates.
Abbreviations: DOL = diagonal orbit length; MOL = maximum orbit length; OD = orbit depth.

The results of our classification tree and logistic regression analyses, both with and without inclusion of phylogenetic information (Tables 7 and 8), indicate that it is feasible to use bony orbit dimensions to determine DAP in a group of mammals without *a priori* designation of groupings within the model. The fact that inclusion of all variables, including multiple body size proxies, increases the accuracy of DAP identification (Tables 7 and 8) suggests the possibility of a body size effect. However, there is not a significant difference in body size among DAP groups (two-sample t tests, $P > 0.45$ for all four body size proxies). It is interesting to note that when considering each orbit measurement individually (DOL, MOL, and IOW), there also is no significant difference among DAP groups (two-sample t tests, $P > 0.15$ for all measurements). The lack of a single-measurement that distinguished DAP groups further indicates that the full suite of measurements is what provides the best DAP signal. DAP has been inferred using pFDA and osteological correlates in a variety of fossil amniotes that possess scleral rings (Schmitz and Motani, 2011a; Angielczyk and Schmitz, 2014). Based on the results of our pFDA analyses compared to our classification trees and logistic regressions, we propose that the latter two methods may be more successful for DAP inference in fossil animals with poorly defined bony orbits. These methods also provide an alternative method for DAP inference in fossil amniotes whose well-defined orbits or scleral rings are frequently damaged or lost during preservation. However, in addition to using comparative taxa that are closely related to the fossil animals under study whenever possible, the complexity of the mammalian skull and its many morphological signals (e.g., influence of masticatory muscle size and attachment, braincase size and morphology) should be considered when making DAP inferences across phylogenetically broad groupings.

ACKNOWLEDGEMENTS

The authors thank L. Heaney, B. Patterson, and the late W. Stanley for facilitating access to the FMNH mammalogy collection.

Literature Cited

Abaño TR, Carig HF, Taraya RL, Ibañez JC. 2011. Participatory resource assessment of the Obu-Manuvu ancestral domain at Sitio Mabanlas, Barangay Carmen, Baguio District, Davao City: field survey report. Davao City, Philippines: Research and Conservation Department, Philippine Eagle Foundation.

Angielczyk KD, Schmitz L. 2014. Nocturnality in synapsids predates the origin of mammals by over 100 million years. Proc R Soc B Biol Sci 281(1793):20141642.

Best TL. 1995. Sciurus oculatus. Mammalian Species 23:1–3.

Bininda-Emonds ORP, Cardillo M, Jones KE, MacPhee RDE, Beck RMD, Grenyer R, Price SA, Vos RA, Gittleman JL, Purvis A. 2007. The delayed rise of present-day mammals. Nature 446: 507–512.

Breiman L, Friedman JH, Olshen RA, Stone CJ. 1984. Classification and regression trees. Boca Raton, FL: Chapman and Hall/CRC.

Brooke M, Hanley S, Laughlin SB. 1999. The scaling of eye size with body mass in birds. Proc R Soc B Biol Sci 266:405–412.

Changizi MA, Shimojo S. 2008. "X-ray vision" and the evolution of forward-facing eyes. J Theor Biol 254:756–767.

Chua MA, Baker N, Yeo RK, Sivasothi N. 2013. New locality records for two species of flying squirrels (Mammalia: Rodentia: Sciuridae) in Singapore. Nat Singapore 6:301–305.

Clement RA. 2004. A quantitative description of lens eye morphology and its implications. Ophthalmic Physiol Opt 24:242–245.

Ferron J. 1976. Comfort behavior of the red squirrel (*Tamiasciurus hudsonicus*). Z Tierpsychol 42:66–85.

Freckleton RP. 2009. The seven deadly sins of comparative analysis. J Evol Biol 22:1367–1375.

Hall MI. 2008a. The anatomical relationships between the avian eye, orbit and sclerotic ring: implications for inferring activity patterns in extinct birds. J Anat 212:781–794.

Hall MI. 2008b. Comparative analysis of the size and shape of the lizard eye. Fortschr Zool 11:62–75.

Hall MI. 2009. The relationship between the lizard eye and associated bony features : a cautionary note for interpreting fossil activity patterns. Anat Rec 292:798–812. https://doi.org/10.1002/ar.20889.

Hall MI, Ross CF. 2007. Eye shape and activity pattern in birds. J Zool 271:437–444.

Hall MI, Kamilar JM, Kirk EC. 2012. Eye shape and the nocturnal bottleneck of mammals. Proc R Soc B Biol Sci 279: 4962–4968.

Hansen TF. 1997. Stabilizing selection and the comparative analysis of adaptation. Evolution 51:1341–1351.

Heesy CP. 2004. On the relationship between orbit orientation and binocular visual field overlap in mammals. Anat Rec 281A: 1104–1110. https://doi.org/10.1002/ar.a.20116.

Heesy CP. 2008. Ecomorphology of orbit orientation and the adaptive significance of binocular vision in primates and other mammals. Brain Behav and Evol 71:54–67.

Heesy CP, Ross CF. 2001. Evolution of activity patterns and chromatic vision in primates: morphometrics, genetics and cladistics. J Hum Evol 40:111–149.

Helgen KM, Cole FR, Helgen LE, Wilson DE. 2009. Generic revision in the holarctic ground squirrel genus *Spermophilus*. J Mammal 90:270–305.

Herring SW, Rafferty KL, Liu ZJ, Lemme M. 2011. Mastication and the postorbital ligament:dynamic strain in soft tissues. Integr Comp Biol 51:297–306.

Ho LST, Ane C. 2014. A linear-time algorithm for Gaussian and non-Gaussian trait evolution models. Syst Biol 63:397–408.

Jessen TG, Kilanowski AL, Gwinn RN, Merrick MJ, Koprowski JL. 2016. *Microsciurus flaviventer* (Rodentia: Sciuridae). Mammalian Species 48:59–65.

Julliot C, Cajani S, Gautier-Hion A. 1998. Anomalures (Rodentia, Anomaluridae) in central Gabon: species composition, population densities and ecology. Mammalia 62:9–22.

Kay RF, Cartmill M. 1977. Cranial morphology and adaptations of *Palaechthon nacimienti* and other Paromomyidae (Plesiadapoidea,? Primates), with a description of a new genus and species. J Hum Evol 6:19–32. IN5, 33–53.

Kay RF, Kirk EC. 2000. Osteological evidence for the evolution of activity pattern and visual acuity in primates. Am J Phys Anthropol 113:235–262.

Kirk EC. 2004. Comparative morphology of the eye in primates. Anat Rec 281:1095–1103.

Kirk EC. 2006. Effects of activity pattern on eye size and orbital aperture size in primates. J Hum Evol 51:159–170.

Kronfeld-Schor N, Dayan T. 2003. Partitioning of time as an ecological resource. Annu Rev Ecol Evol Syst 34:153–181.

Land MF. 1981. Optics and vision in invertebrates. In: Land MF, Laughlin SB, Naessel DR, Strausfeld NJ, Waterman TH, editors. Comparative physiology and evolution of vision in invertebrates B: invertebrate visual centers and behavior I. Berlin, Heidelberg, New York: Springer-Verlag. p 471–592.

Lythgoe JN. 1979. The ecology of vision. Oxford: Clarendon Press.

MacIver MA, Schmitz L, Mugan U, Murphey TD, Mobley CD. 2017. Massive increase in visual range preceded the origin of terrestrial vertebrates. Proc Natl Acad Sci USA 114: E2375–E2384.

Martin GR. 1983. Schematic eye models in vertebrates. Prog Sens Physiol 4:43–81.

Milborrow S. 2016. rpart.plot: Plot rpart Models. An Enhanced Version of plot.rpart. R Package. http://CRAN.R-project.org/package=rpart.plot

Molur S, Srinivasulu C, Srinivasulu B, Walker S, Nameer PO, Ravikumar L. 2005. Status of south Asian non-volant small mammals: conservation assessment and management plan (CAMP) workshop report. Coimbatore, India: Zoo Outreach Organization/CBSG-South Asia.

Motani R, Schmitz L. 2011. Phylogenetic versus functional signals in the evolution of form–function relationships in terrestrial vision. Evolution 65:2245–2257.

Nowak RM. 1999. Walker's Mammals of the World, Vol. 1. Baltimore: JHU Press.

Pihlström H. 2012. The size of major mammalian sensory organs as measured from cranial characters and their relation to the biology and evolution of mammals. PhD. Dissertation.

R Core Team. 2016. R: A language and environment for statistical computing. Vienna, Austria: R Foundation for Statistical Computing.

Revell LJ. 2012. phytools: an R package for phylogenetic comparative biology (and other things). Methods Ecol Evol 3:217–223.

Roll U, Dayan T, Kronfeld-Schor N. 2006. On the role of phylogeny in determining activity patterns of rodents. Evol Ecol 20:479–490.

Rosenberger AL, Smith TD, DeLeon VB, Burrows AM, Schenck R, Halenar LB. 2016. Eye size and set in small–bodied fossil primates: a three-dimensional method. Anat Rec 299:1671–1689.

Ross CF. 2000. Into the light: the origin of Anthropoidea. Ann Rev Anthropol 29:147–194.

Ross CF, Hall MI, Heesy CP. 2007. Were basal primates nocturnal? Evidence from eye and orbit shape. Primate origins: adaptations and evolution. New York: Springer. p 233–256.

Ross CF, Kirk EC. 2007. Evolution of eye size and shape in primates. J Hum Evol 52:294–313.

Schmitz L. 2009. Quantitative estimates of visual performance features in fossil birds. J Morphol 270:759–773.

Schmitz L, Motani R. 2010. Morphological differences between the eyeballs of nocturnal and diurnal amniotes revisited from optical perspectives of visual environments. Vision Res 50:936–946.

Schmitz L, Motani R. 2011a. Nocturnality in dinosaurs inferred from scleral ring and orbit morphology. Science 332:705–708.

Schmitz L, Motani R. 2011b. Response to comment on "Nocturnality in dinosaurs inferred from scleral ring and orbit morphology.". Science 334:1641.

Schmitz L, Wainwright PC. 2011. Ecomorphology of the eyes and skull in zooplanktivorous labrid fishes. Coral Reefs 30:415–428.

Schoener TW. 1974. Resource partitioning in ecological communities. Science 185:27–39.

Schultz AH. 1940. The size of the orbit and of the eye in Primates. Am J Phys Anthropol 26:389–408.

Therneau TM, Atkinson EJ. 2017. An introduction to recursive partitioning using the RPART routines. R package. https://cran.r-project.org/web/packages/rpart/vignettes/longintro.pdf

Thomas R, Kelly D, Goodship N. 2004. Eye design in birds and visual constraints on behavior. Ornitol Neotrop 15:243–250.

Thomas RJ, Székely T, Cuthill IC, Harper DGC, Newson SE, Frayling TD, Wallis PD. 2002. Eye size in birds and the timing of song at dawn. Proc Biol Sci 269:831–837.

Thomas RJ, Székely T, Powell RF, Cuthill IC. 2006. Eye size, foraging methods and the timing of foraging in shorebirds. Funct Ecol 20:157–165.

Thorington RW Jr, Koprowski JL, Steele MA, Whatton JF. 2012. Squirrels of the world. Baltimore, MD: JHU Press.

Werner YL, Seifan T. 2006. Eye size in geckos : asymmetry, allometry, sexual dimorphism, and behavioral correlates. J Morphol 267: 1486–1500.